Materials Science Forum Vols. 492-493 (2005) pp 447-452
Online available since 2005/Aug/15 at www.scientific.net

doi:10.4028/www.scientific.net/MSF.492-493.447

Dynamic Fracture of Functionally Graded Composites Using an Intrinsic Cohesive Zone Model

Glaucio H. Paulino[1,a] and Zhengyu Zhang[2,b]

[1]Department of Civil and Environmental Engineering, University of Illinois at Urbana-Champaign, Newmark Laboratory, 205 North Mathews Avenue, Urbana, IL 61801, U.S.A.

[2]Department of Civil and Environmental Engineering, University of Illinois at Urbana-Champaign, Newmark Laboratory, 205 North Mathews Avenue, Urbana, IL 61801, U.S.A.

[a]paulino@uiuc.edu, [b] zzhang3@uiuc.edu

Keywords: Finite element method, graded finite element, functionally graded material (FGM), intrinsic cohesive zone model (CZM), dynamics, fracture, branching.

Abstract. This paper presents a Cohesive Zone Model (CZM) approach for investigating dynamic failure processes in homogeneous and Functionally Graded Materials (FGMs). The failure criterion is incorporated in the CZM using both a finite cohesive strength and work to fracture in the material description. A novel CZM for FGMs is explored and incorporated into a finite element framework. The material gradation is approximated at the element level using a graded element formulation. A numerical example is provided to demonstrate the efficacy of the CZM approach, in which the influence of the material gradation on the crack branching pattern is studied.

Introduction

Compared to the classical linear elastic fracture mechanics (LEFM) and some other existing fracture models, Cohesive Zone Models (CZMs) provide advantages of allowing spontaneous crack nucleation, crack branching and fragmentation, as well as crack propagation without an external fracture criterion [1, 2].

CZMs incorporate a cohesive strength and finite work to fracture in the description of material behavior, and allow simulation of near-tip behavior and crack propagation. The concept of "cohesive failure" is illustrated in Figure 1, in which a *cohesive zone*, along the plane of potential crack propagation, is present in front of the crack tip. Within the extent of the cohesive zone, the material points which were identical when the material was intact, separate to a distance Δ due to influence of high stress state at the crack tip vicinity. The cohesive zone surface sustains a distribution of tractions T which are function of the displacement jump across the surface Δ, and the relationship between the traction T and separation Δ is defined as the constitutive law for the cohesive zone surface. For intrinsic CZM as employed in this study, the traction T first increases with increasing interfacial separation Δ, reaches a maximum value δ, then decreases and finally vanishes at a characteristic separation value δ_c, where complete decohesion is assumed to occur.

The CZM approach has the promise of simulating fracture process where cracking occurs spontaneously. The fracture path and speed become natural outcome of the simulation rather than being specified *ad hoc* or *a priori*. In this paper, a novel cohesive zone model developed for

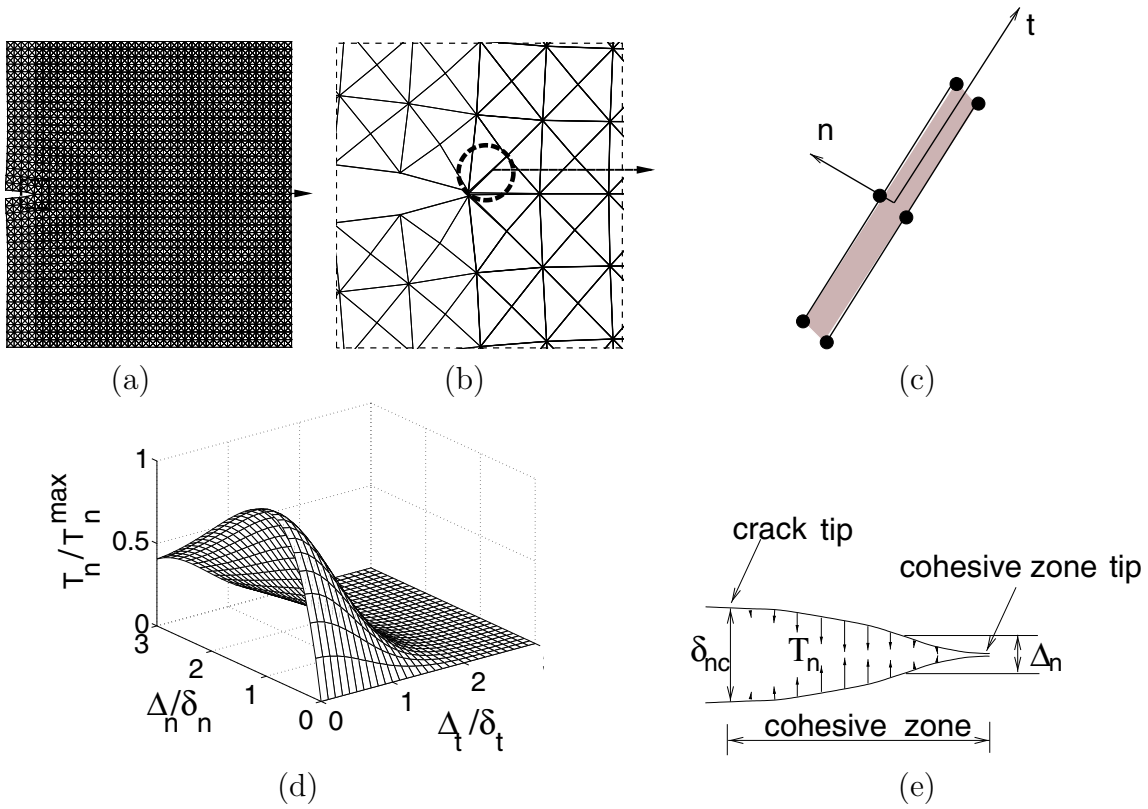

Fig. 1: Schematic representation of cohesive zone model concept; (a) A plate containing crack; At potential crack propagation path *e.g.*, as circled in (b), cohesive element is inserted, as shown in (c), which follows the specified cohesive zone model shown in (d) for normal traction; (e) cohesive zone in Mode I case.

Numerical Scheme

This section briefly outlines the essential components of the numerical scheme, namely, the FEM framework incorporating CZM, the dynamic updating scheme and the material gradation.

To incorporate a CZM into the numerical scheme for dynamic fracture, the *cohesive element* is developed and positioned along the potential path or region of crack propagation, and attached to the volumetric elements, which follows a cohesive *traction-separation* relationship as shown in Figure 1. In contrast, the conventional finite element, which is now called "*bulk* element", follows conventional *stress-strain* relationships (continuum description). The constitutive law of cohesive elements is inherently embedded in the finite element model, so that the presence of cohesive elements allows spontaneous crack propagation.

The FEM formulation incorporating cohesive elements is derived from the principle of virtual work, and discretized using the explicit central difference time stepping scheme to update displacements $\mathbf{u}$, accelerations $\ddot{\mathbf{u}}$ and velocities $\dot{\mathbf{u}}$ as follows:

$$\mathbf{u}_{n+1} = \mathbf{u}_n + \Delta t \dot{\mathbf{u}}_n + \frac{1}{2}\Delta t \ddot{\mathbf{u}}_n \tag{1}$$

$$\ddot{\mathbf{u}}_{n+1} = \mathbf{M}^{-1}(\mathbf{F} + \mathbf{R}_{int_{(n+1)}} - \mathbf{R}_{coh_{(n+1)}}) \tag{2}$$

$$\dot{\mathbf{u}}_{n+1} = \dot{\mathbf{u}}_n + \frac{\Delta t}{2}(\ddot{\mathbf{u}}_n + \ddot{\mathbf{u}}_{n+1}) \tag{3}$$

where Δt denotes the time step, $\mathbf{M}$ is the lumped mass matrix, $\mathbf{F}$ is the external force vector, $\mathbf{R}_{int}$ and $\mathbf{R}_{coh}$ are the global internal and cohesive force vectors, which are obtained from

the contribution of *bulk* and *cohesive* elements, respectively. Large deformation formulation is employed [3].

To treat the material nonhomogeneity inherent in the problem, *graded elements*, which incorporate the material property gradient at the element level, are introduced. In this investigation, the scheme proposed by Kim and Paulino [4] is adopted. The same shape functions are used to interpolate the unknown displacements, the geometry, and the material parameters, and thus the interpolations for material properties (E, ν, ρ) are given by $E = \sum_{i=1}^{m} N_i E_i, \nu = \sum_{i=1}^{m} N_i \nu_i, \rho = \sum_{i=1}^{m} N_i \rho_i$, where N_i are the standard shape functions.

Cohesive Zone Model for FGMs

We propose a new FGM cohesive zone model [3], which is a combination of the models by Xu and Needleman [1] and Jin *et al.* [5]. It avoids effective quantities and thus uses the actual quantities to describe the relationship between normal traction-separation and tangential traction-separation.

Assume that the energy potential of each individual material phase takes the exponential form [1]:

$$\phi_i(\boldsymbol{\Delta}) = \phi_{ni} + \phi_{ni} \exp\left(-\frac{\Delta_n}{\delta_{ni}}\right) \left\{ \left[1 - r_i + \frac{\Delta_n}{\delta_{ni}}\right] \frac{(1-q_i)}{(r_i-1)} - \left[q_i + \frac{(r_i-q_i)}{(r_i-1)} \frac{\Delta_n}{\delta_{ni}}\right] \exp(-\frac{\Delta_t^2}{\delta_{ti}^2}) \right\} \tag{4}$$

in which superscripts i $(i = 1, 2)$ denote the two individual material phases (*e.g.*, metal and ceramic respectively), and parameters $\boldsymbol{\Delta} = [\Delta_n, \Delta_t]$ denote the displacement jump across the cohesive surface in normal and tangential directions. Other parameters in the expressions that respectively refer to material phase i are explained hereby without subscript notation: parameters ϕ_n and ϕ_t are the energies required for pure normal and tangential separation, respectively; δ_n and δ_t are the critical opening displacement for normal and tangential separation, which are related to the cohesive normal strength $T_n^{\max}$ and tangential strength $T_t^{\max}$ as $\phi_n = eT_n^{\max}\delta_n, \phi_t = \sqrt{e/2}T_t^{\max}\delta_t$, $q = \phi_t/\phi_n$, and r is defined as the value of Δ_n/δ_n after complete shear separation with $T_n = 0$.

The cohesive traction force vectors associated with material phases 1 and 2 in the 2-D case comprise traction in normal and tangential directions as $\mathbf{T}_1 = [T_{n1}, T_{t1}]$, $\mathbf{T}_2 = [T_{n2}, T_{t2}]$, and can be derived directly from the energy potentials as $\mathbf{T}_1 = -\partial\phi_1/\partial\boldsymbol{\Delta}, \mathbf{T}_2 = -\partial\phi_2/\partial\boldsymbol{\Delta}$. The resulting normal and shear traction components are illustrated in Figure 2 (a).

Let $\mathbf{T}_{\text{FGM}} = \left[T_n^{\text{FGM}}, T_t^{\text{FGM}}\right]$ denote the traction force vector across the cohesive surfaces of a two-phase FGM, which comprises normal and tangential traction force components. The cohesive traction $\mathbf{T}_{\text{FGM}}$ is approximated by the following volume fraction based formula

$$\mathbf{T}_{\text{FGM}}(\mathbf{x}) = \frac{V_1(\mathbf{x})}{V_1(\mathbf{x}) + \beta_1[1 - V_1(\mathbf{x})]}\mathbf{T}_1 + \frac{1 - V_1(\mathbf{x})}{1 - V_1(\mathbf{x}) + \beta_2 V_1(\mathbf{x})}\mathbf{T}_2 \tag{5}$$

where the parameter $V_1(\mathbf{x})$ denotes volume fraction of the material phase 1, while β_1 and β_2 are two cohesive gradation parameters that describe the transition of failure mechanisms from pure material phase 1 to pure material phase 2, and should be calibrated with experimental data. Figure 2 (b) compares the normal traction-separation laws for two material constituents.

Numerical Example

In this section, a test example is provided to illustrate the application of the cohesive model introduced above to both homogeneous and FGM systems through investigation of dynamic

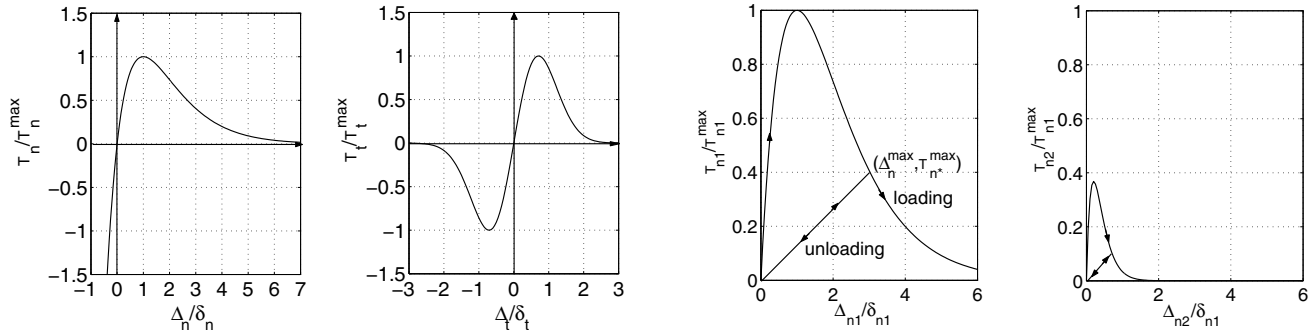

(a) (b)

Fig. 2: (a) Exponential cohesive zone model [1] in pure tension and pure shear; (b) cohesive zone model in pure tension case, for two material phases with strength ratio $T_{n2}^{max}/T_{n1}^{max} = 0.35$, and critical displacement ratio $\delta_{n2}/\delta_{n1} = 0.15$, where δ_{ni} denotes normal separation at peak normal traction for material i.

crack branching phenomenon for a plane strain plate containing an initial central crack subjected to tensile velocity loading.

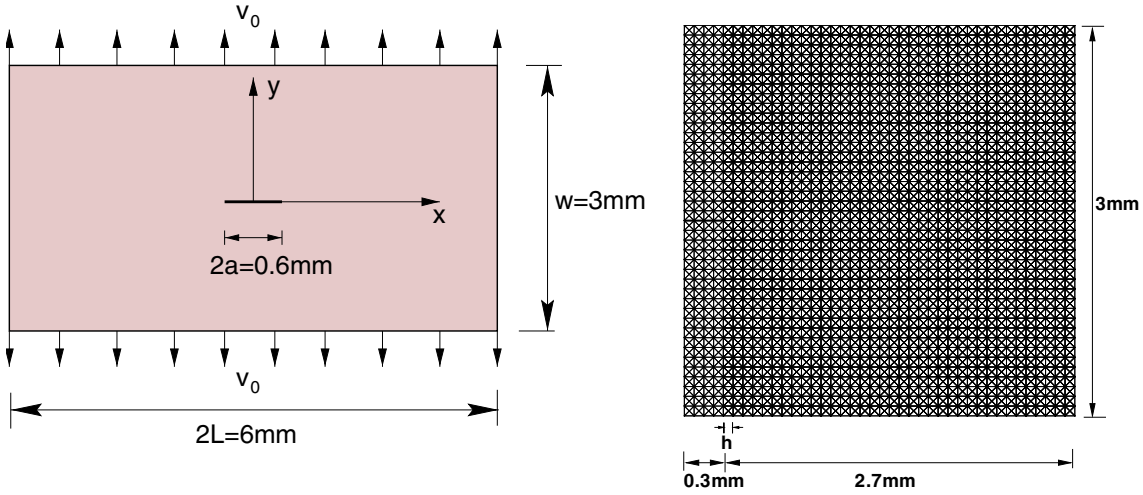

(a) (b)

Fig. 3: Branching problem; (a) geometry and boundary conditions of a plate containing a central crack subjected to velocity loading; (b) Mesh descretization of the dynamic branching problem with half of the original geometry modelled due to symmetry along the y axis.

Problem Description. The computation is carried out for a center cracked rectangular plate as shown in Figure 3 (a). Symmetric velocity loading $v_0 = 5m/s$ is applied along the upper and lower surfaces. To explore the influence of material gradation on crack branching patterns, three material gradation profiles are studied, as listed in Table 1: *case 1*: both the bulk and cohesive properties are considered for homogeneous materials; *case 2*: hypothetical "FGM", with homogeneous bulk material and linearly graded cohesive properties along y direction. *case 3*: FGM with both the bulk and cohesive properties linearly graded in y direction.

Due to symmetry of the geometry, material gradation and loading condition with respect to y axis, only the right half of the geometry is modelled for the numerical simulation, along with proper boundary condition to account for the symmetry at $x = 0$. The domain is discretized

with 40 by 40 quads each divided into 4 T3 elements, as depicted in Figure 3 (b). Cohesive elements are inserted inside a rectangular region right to the initial crack, as shown with the thicker lines. The other material parameters for the CZM are: $q = 1, r = 0, and\ \beta_1 = \beta_2 = 1$.

Table 1: Three material gradation profiles for plate containing central crack.

	y position	E (GPa)	ν	ρ (kg/m^3)	G_{Ic} (N/m)	$T_{\max}$ (MPa)	δ_c (μm)
case 1: homog.	$-1/2W$ to $1/2W$	3.24	0.35	1190	352.3	324	0.4
case 2: graded T_{max}	$1/2W$	3.24	0.35	1190	528.4	486	0.4
	$-1/2W$	3.24	0.35	1190	176.1	162	0.4
case 3: graded E & T_{max}	$1/2W$	4.86	0.35	1190	528.4	486	0.4
	$-1/2W$	1.62	0.35	1190	176.1	162	0.4

Results for Various Material Gradation Profiles. *Case 1: homogeneous PMMA material.* Symmetric branch pattern is obtained (Figure 4 (a)). The crack begins to branch at $a_{branch} = 1.05mm$, and further branches occur when the cracks approach the edge. Although crack branching can only take place either parallel to the coordinate axes or at $\pm 45°$, the overall branching angle is less than 45° from the x axis. In the example, the overall branching angle is about 29°, calculated by approximating the main branch as a straight line.

Case 2: Variation of cohesive strength. In this example, the cohesive strength T_{max} is lower at the bottom surface and higher at the top surface, which means weaker fracture resistance at the lower region. Therefore, the crack branching is expected to be more significant at the lower part of the plate, as shown in Figure 4(b). The initial crack branching location is roughly the same as the homogeneous case (Figure 4(c)), yet it disappears in the final figure (Figure 4(b)). As the lower region of the plate is weaker in resisting fracture, the crack branch towards the lower region dominates, and shields the upward one from developing further.

Case 3: Graded bulk and cohesive properties. In this example, both bulk and cohesive properties vary linearly in y direction. On one hand, the weaker cohesive resistance favors the crack branching into the $y < 0$ region. On the other hand, stress developed in the stiffer region ($y > 0$) is higher than that at the compliant region, which may promote the crack branching into the $y > 0$ region. These two mechanisms compete with each other in influencing crack branching pattern. The final crack pattern is plotted in Figure 4 (d).

Conclusions

This paper presents a numerical scheme incorporating CZM to investigate dynamic fracture behavior of homogeneous and FGMs under dynamic loading. Two basic types of elements are employed in the present investigation: *graded* elements in the bulk material, and *graded intrinsic cohesive* elements to model fracture. Xu and Needleman [1] model was extended to treat FGMs, which eliminates the dependence upon effective quantities, and may provide certain advantages when mixed-mode effect is prominent. As illustrated in the study, the cohesive element approach is promising for modeling generalized fracture without predefined external fracture criteria. Further numerical issues, including the artificial compliance introduced in the system by incorporating cohesive elements, are studied and related results are reported in recent publication by the authors [3].

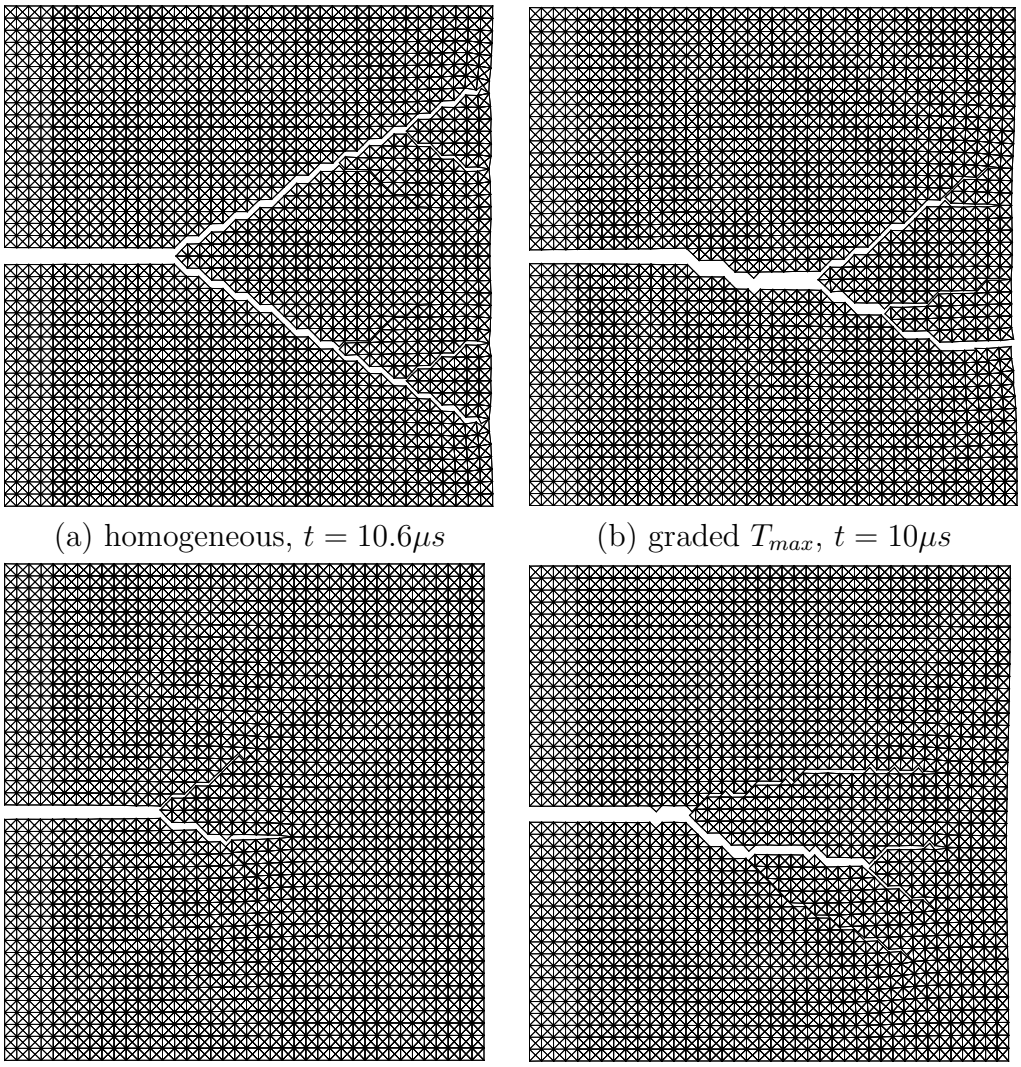

(a) homogeneous, $t = 10.6\mu s$ (b) graded T_{max}, $t = 10\mu s$

(c) graded T_{max}, $t = 8.25\mu s$ (d) graded E and T_{max}, $t = 10\mu s$

Fig. 4: Crack branch pattern for various material gradation profiles; loading velocity at $v_0 = 5m/s$; (a) final crack pattern at $t = 10.6\mu s$ for homogeneous plate (case 1); (b) final crack pattern at $t = 10\mu s$ for graded plate (case 2); (c) attempted crack branching at $t = 8.25\mu s$ for graded plate (case 2); (d) final crack pattern at $t = 10\mu s$ for graded plate (case 3).

References

[1] X. Xu, A. Needleman: International Journal of Fracture Vol. 74 (1995), p. 289-324.

[2] G.T. Camacho, M. Ortiz: International Journal of Solids and Structures Vol. 33 (1996), p. 2899-2938.

[3] Z. Zhang, G.H. Paulino: International Journal of Plasticity, (accepted, 2004).

[4] J.H. Kim, G.H. Paulino: ASME Journal of Applied Mechanics, Vol. 69 (2002), p. 502-514.

[5] Z.-H. Jin, G.H. Paulino, R.H. Dodds, Jr.: ASME Journal of Applied Mechanics, Vol. 69 (2002), p. 370-379.

Functionally Graded Materials VIII
doi:10.4028/www.scientific.net/MSF.492-493

Dynamic Fracture of Functionally Graded Composites Using an Intrinsic Cohesive Zone Model

doi:10.4028/www.scientific.net/MSF.492-493.447